Available online at www.sciencedirect.com
SCIENCE DIRECT®
Journal of Solid State Chemistry 177 (2004) 4237–4243
JOURNAL OF SOLID STATE CHEMISTRY
www.elsevier.com/locate/jssc

Rh_3B_{2-x}, new structure type of binary borides with triclinic symmetry

P. Salamakha[a], O. Sologub[a,b,*], C. Rizzoli[c], A.P. Gonçalves[a], M. Almeida[a]

[a]*Departamento de Química, Instituto Tecnològico e Nucleare, Estrada Nacional 10, P-2686-953 Sacavèm, Portugal*
[b]*Institut für Anorganische Chemie, Universität Wien, Währingerstrasse 42, A-1090 Wien, Austria*
[c]*Dipartimento di Chimica GIAF, Università di Parma, Viale delle Scienze 17/A, I-43100 Parma, Italy*

Received 16 April 2004; received in revised form 18 June 2004; accepted 24 June 2004

Abstract

New binary compound Rh_3B_{2-x}, $x = 0.167$ crystallizing with its own structure type has been observed from the as cast alloys. The compound has a limited thermal stability range: it was found to decompose after annealing at 800 °C for 20 days. The crystal structure was investigated by X-ray diffraction from two single crystals using different techniques: CAD-4 automatic diffractometer, $a = 5.470(2)$, $b = 6.816(3)$, $c = 9.068(4)$, $\alpha = 110.74(3)$, $\beta = 94.81(3)$, $\gamma = 90.44(2)$, 107 refined parameters, $R_1 = 0.0418$, $wR_2 = 0.1087$ for 1223 reflections with $I > 2\sigma(I_o)$, and BRUKER SMART AXS, $a = 5.483(4)$, $b = 6.818(6)$, $c = 9.072$ (7), $a = 110.78(1)$, $b = 94.73(1)$, $g = 90.46(1)$, 107 refined parameters, $R_1 = 0.0401$, $wR_2 = 0.0959$ for 943 reflections with $I > 2\sigma(I_o)$. The Rh_3B_{2-x}, structure (space group $P\bar{1}$, Pearson symbol $aP30-1$) is the first representative of structures with triclinic symmetry among binary borides and contains three different types of boron-boron aggregation: isolated boron atoms, B–B pairs and B_6 chain fragments.
© 2004 Elsevier Inc. All rights reserved.

1. Introduction

The formation and crystal structures of the binary Rh–B compounds were studied in a course of our systematic investigations of the Ce(Y)–Rh–B ternary systems. The schematic Rh–B phase diagram is presented in Ref. [1], which is based on the melting points of two compounds, $RhB_{1.1}$ and Rh_7B_3 [2] and Rh-rich eutectic temperature [3]. According to Ref. [4], these compounds belong to anti-NiAs ($P6_3/mmc$ space group, $a = 3.3058$ Å, $c = 4.2094$ Å) and Th_7Fe_3 ($P6_3mc$ space group, $a = 7.471$ Å, $c = 4.777$ Å) structure types, respectively. The authors of Refs. [5,6] reported on the results of single crystal structural investigations for two more compounds Rh_2B ($Pnma$ space group, $a = 5.42$ Å, $b = 3.98$ Å, $c = 7.44$ Å) and Rh_5B_4 ($P6_3/mmc$ space group, $a = 3.3058$ Å, $c = 20.394$ Å).

From our investigations by means of X-ray powder and single crystal diffraction of the as cast and annealed at 800 °C Rh–B samples, the existence of the Rh_7B_3, Rh_5B_4 and $RhB_{1.1}$ compounds have been confirmed. The Rh_2B compound has not been observed. New binary boride Rh_3B_{2-x}, $x = 0.166$ was observed in the as cast samples and found to decompose after annealing at 800 °C. In the presented paper we report on the result of the X-ray single crystal investigation of this phase. Detailed description of the results of the investigation of the Rh–B phase diagram will be a subject of our forthcoming publication.

2. Experimental details

2.1. Synthesis

The Rh–B binary alloys with different composition and a total weight of 0.5 g, were synthesized by arc melting proper amounts of the constituent elements under high purity argon on a water cooled copper hearth. The purities of the starting materials were not less than 99.9% for boron obtained from CHEMPUR, Germany and 99.95% for rhodium (ÖGUSSA-Wien, Austria). The melting procedure was repeated at least

*Corresponding author.
E-mail address: salamakh@mail.lviv.ua (O. Sologub).

0022-4596/$ - see front matter © 2004 Elsevier Inc. All rights reserved.
doi:10.1016/j.jssc.2004.06.040

three times in order to ensure a better homogeneity, with total weight losses less than 1%. The resulting ingots were then sealed under vacuum into silica tubes and annealed for 20 days at 800 °C, followed by quenching into cold water.

2.2. X-ray powder diffraction

The as-cast and annealed samples were examined by X-ray powder diffraction. Diffracted X-ray intensities were collected from the powdered "as cast" and annealed samples at room temperature with a Image Plate Huber G670 camera ($20 \leqslant 2\theta \leqslant 100°$, step size 0.005°, exposure time 24 h) with monochromic Cu$K_{\alpha 1}$ ($\lambda = 1.54056$ Å) radiation. Phase identification, automatic indexing and lattice parameters refinement were accomplished using the WinPlotr [7], Powder Cell [8], TREOR [9] and DICVOL [10] programs.

2.3. Single crystal X-ray diffraction

Single crystals suitable for the X-ray measurements were isolated by mechanical fragmentation from the buttons of the "as cast" $Rh_{0.67}B_{0.33}$ and $Rh_{0.60}B_{0.40}$ alloys, glued on the top of a glass fiber and mounted on to the goniometer head. X-ray single crystal diffraction data for the crystal **I,** which was selected out from the $Rh_{0.67}B_{0.33}$ sample, were obtained using a four circle diffractometer Enraf-Nonius CAD-4 with graphite monochromatized MoK_α radiation ($\lambda = 0.71073$ Å). The data set was recorded at 20 °C in a $\omega - 2\theta$ scan mode. The intensities were corrected for absorption (using *psi-scan*), polarization and Lorentz effect.

For the single crystal **II** isolated out from the $Rh_{0.60}B_{0.40}$ alloy, the X-ray diffraction data were obtained using a Bruker AXS CCD diffractometer (graphite monochromatized MoK_α radiation, $\lambda = 0.71073$ Å). The data set was recorded at 27 °C in the ω-scan mode. A total of 2424 frames were collected with a $\Delta\varphi$ of 0.3° and an exposure time of 30 s. Data reduction was carried out using the SAINT suite of programs [11]. The intensities were corrected for absorption with the assistance of the program SADABS [11].

Further details of single crystal data collection and structural refinement for both crystals are listed in Table 2.

3. Results

3.1. X-ray phase analysis

The existence of the Rh_7B_3, Rh_5B_4 and $RhB_{1.1}$ compounds have been confirmed from the phase analysis of the as cast and annealed at 800 °C Rh–B samples. The crystallographic characteristics obtained for these phases agree well with those reported in Refs. [2,6]. The sample of the $Rh_{0.67}B_{0.33}$ composition which corresponds to the earlier reported "Rh_2B" compound [5] was found to contain two phases in both annealed at 800 °C (namely Rh_7B_3 and Rh_5B_4) and as cast conditions (Rh_7B_3 and phase with unknown structure) (Table 1). The X-ray powder pattern of the $Rh_{0.60}B_{0.40}$ sample revealed mainly the reflections belonging to the unknown phase, which was consequently investigated by X-ray single crystal diffraction.

3.2. X-ray single crystal structural study

The lattice parameters for the crystal **I** ($a = 5.470(2)$ Å, $b = 6.816(3)$ Å, $c = 9.068(4)$ Å, $\alpha = 110.74(3)°$, $\beta = 94.81(3)°$, $\gamma = 90.44(2)°$) were obtained from the automatic indexing and the least-square refinement of the 25 well-centered and strong reflections measured in the various regions of the reciprocal space and for the crystal **II** ($a = 9.072(7)$ Å, $b = 6.818(6)$ Å, $c = 5.483(4)$ Å, $\alpha = 90.46(1)$, $\beta = 85.27(1)$, $\gamma = 69.22(1)$ from automatic indexing and least-square refinement of 242 reflections.

For the analyses of the X-ray single crystal data and structure refinement, the WinGX 1.64 program package [12] was used. The presence of a center of symmetry and the space group was checked using the procedure E-STATS [13] and ABSEN [14]. The structure was solved

Table 1
Results of the X-ray phase analyses for the selected samples of the Rh–B system

Nominal composition	Heat treatment, °C	Phase analyses	Space group	Structure type	Lattice parameters, Å	
					a	*c*
$Rh_{0.67}B_{0.33}$	As cast	Rh_7B_3	$P6_3mc$	Th_7Fe_3	7.4702(2)	4.7759(1)
		Unknown (traces)				
$Rh_{0.67}B_{0.33}$	800	Rh_7B_3	$P6_3mc$	Th_7Fe_3	7.4707(2)	4.7736(2)
		Rh_5B_4	$P6_3/mmc$	Rh_5B_4	3.3057(3)	20.386(9)
$Rh_{0.60}B_{0.40}$	As cast	Unknown				
$Rh_{0.60}B_{0.40}$	800	Rh_7B_3	$P6_3mc$	Th_7Fe_3	7.4736(3)	4.7759(3)
		Rh_5B_4	$P6_3/mmc$	Rh_5B_4	3.3063(2)	20.393(8)

Table 2
Parameters for the single crystal X-ray data collection and refinement

Crystal	I	II
Diffractometer	CAD-4	Bruker SMART AXS
Lattice parameters, Å		
a	5.470(2)	5.483(4)
b	6.816(3)	6.818(6)
c	9.068(4)	9.072(7)
α (deg)	110.74(3)	110.78(1)
β (deg)	94.81(3)	94.73(1)
γ (deg)	90.44(2)	90.46(1)
Cell volume, Å^3	314.8(2)	315.7(4)
Calculated density, g cm^{-3}	10.398	10.367
Linear absorption coefficient (mm^{-1})	22.84	22.84
$2\theta_{max}$	53.92	50.13
Data set	$-6\leqslant h\leqslant 6$, $-8\leqslant k\leqslant 8$, $-11\leqslant l\leqslant 11$	$-6\leqslant h\leqslant 6$, $-8\leqslant k\leqslant 8$, $-10\leqslant l\leqslant 10$
Number of measured reflections	2716	2702
Number of unique reflections	1356 ($R_{int} = 0.0488$)	1113($R_{int} = 0.0338$)
Number of reflections with $I > 2\sigma(I_o)$	1223	943
Number of refined parameters	107	107
R_1, wR_2 ($I > 2\sigma(I_o)$)	0.0418, 0.1087	0.0401, 0.0959
R_1, wR_2 (all data)	0.0467, 0.1115	0.0468, 0.0991
Goodness of fit	1.218	1.014
Extinction coefficient	0.003488(3)	0.000320(1)
Highest/lowest peaks of electron density (e/Å)	2.51/−2.22	2.01/−3.60

Table 3
Atomic coordinates and thermal parameters for the Rh_3B_{2-x} compound

Atom	x	y	z	G, %	$U^*_{eq} \times 10^2$, Å^2
Rh1	0.03916(2)	0.19795(17)	0.48455(14)	100	0.86(3)
Rh2	0.15373(2)	0.44179(17)	0.31144(14)	100	0.85(3)
Rh3	0.76978(2)	0.90099(16)	0.22804(14)	100	0.78(3)
Rh4	0.26047(2)	0.47235(16)	0.02617(13)	100	0.79(3)
Rh5	0.27871(2)	0.85397(17)	0.28168(14)	100	0.80(3)
Rh6	0.53484(2)	0.26034(17)	0.45415(14)	100	0.89(3)
Rh7	0.42598(2)	0.14324(17)	0.12941(14)	100	0.79(3)
Rh8	0.10223(2)	0.81444(17)	0.96631(14)	100	0.87(3)
Rh9	0.65627(2)	0.52488(16)	0.26886(13)	100	0.94(3)
B1	0.016(3)	0.375(2)	0.8086(19)	100	0.7(3)
B2	0.099(3)	0.097(3)	0.221(2)	100	0.9(3)
B3	0.217(3)	0.760(2)	0.729(2)	100	0.8(3)
B4	0.353(3)	0.043(3)	0.544(2)	100	1.0(3)
B5	0.462(3)	0.770(2)	0.0583(19)	100	0.6(3)
B6	0.158(6)	0.527(5)	0.552(4)	50	0.8(6)

*U_{iso} for B atoms.

Table 4
Anisotropic thermal parameters for the Rh atoms in Rh_3B_{2-x} structure

Atom	$U_{11} \times 10^2$, Å^2	$U_{22} \times 10^2$, Å^2	$U_{33} \times 10^2$, Å^2	$U_{23} \times 10^2$, Å^2	$U_{13} \times 10^2$, Å^2	$U_{12} \times 10^2$, Å^2
Rh1	0.92(5)	0.57(5)	1.18(6)	0.35(4)	0.47(4)	0.20(4)
Rh2	0.88(6)	0.68(5)	1.21(6)	0.49(4)	0.50(4)	0.24(4)
Rh3	0.80(5)	0.57(5)	1.12(6)	0.39(4)	0.46(4)	0.21(4)
Rh4	0.90(5)	0.54(5)	1.06(6)	0.37(4)	0.48(4)	0.15(4)
Rh5	0.93(6)	0.60(5)	1.05(6)	0.41(4)	0.49(4)	0.24(4)
Rh6	0.84(5)	0.75(5)	1.12(6)	0.29(4)	0.50(4)	0.17(4)
Rh7	0.79(6)	0.65(5)	1.06(6)	0.36(4)	0.46(4)	0.17(4)
Rh8	0.86(6)	0.67(5)	1.21(6)	0.42(4)	0.44(4)	0.17(4)
Rh9	0.91(6)	0.74(5)	1.18(6)	0.27(4)	0.51(4)	0.19(4)

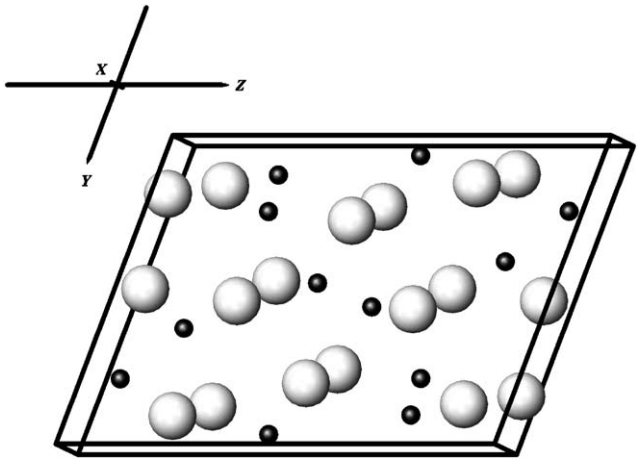

Fig. 1. Projection of the Rh_3B_{2-x}, unit cell on the YZ plane.

with the aid of the SHELXS-97 [15] program in the space group $P\bar{1}$ [16] using the Patterson method, which resulted in the positions of all Rh atoms. Difference Fourier syntheses enabled us to localize the position of the boron atoms. The structure was refined by a full-matrix least square program using atomic scattering factors provided by the program package SHELXL-97 [17]. The weighting schemes included a term, which accounted for the counting statistics, and the parameter correcting for isotropic secondary extinction was optimized. The anisotropic displacement parameters for Rh atoms and the isotropic displacement parameter for the B atom were refined. The refinement showed an approximately ~5 times larger value for the displacement parameter for the B6 atom than for other boron atoms. Consequently, an occupancy of 50% was

Table 5
Selected interatomic distances (d, Å) for the Rh atoms in the Rh_3B_{2-x} structure

Atom	*d*, Å	Atom	*d*, Å	Atom	*d*, Å
Rh1–B4	2.151(16)	Rh4–B1	2.175(16)	Rh7–B2	2.104(16)
Rh1–B6	2.18(3)	Rh4–B5	2.215(15)	Rh7–B5	2.124(15)
Rh1–B6	2.28(3)	Rh4–B1	2.216(16)	Rh7–B3	2.205(16)
Rh1–B2	2.290(17)	Rh4–B5	2.228(15)	Rh7–B5	2.407(15)
Rh1–B3	2.392(16)	Rh4–Rh8	2.7073(18)	Rh7–Rh7	2.660(3)
Rh1–B4	2.629(16)	Rh4–Rh4	2.749(2)	Rh7–Rh2	2.6764(19)
Rh1–Rh2	2.7597(18)	Rh4–Rh3	2.7553(2)	Rh7–Rh9	2.703(2)
Rh1–Rh9	2.771(2)	Rh4–Rh9	2.758(2)	Rh7–Rh8	2.738(2)
Rh1–Rh2	2.778(2)	Rh4–Rh2	2.7765(19)	Rh7–Rh6	2.774(2)
Rh1–Rh3	2.779(2)	Rh4–Rh8	2.7963(18)	Rh7–Rh3	2.8062(18)
Rh1–Rh6	2.7926(18)	Rh4–Rh5	2.799(2)	Rh7–Rh8	2.8352(18)
Rh1–Rh6	2.8001(19)	Rh4–Rh7	2.8468(18)	Rh7–Rh4	2.8468(18)
Rh1–Rh5	2.828(2)	Rh4–Rh9	2.879(2)	Rh7–Rh5	2.9212(18)
Rh2–B6	2.04(3)	Rh5–B1	2.133(15)	Rh8–B5	2.137(15)
Rh2–B1	2.10(15)	Rh5–B2	2.140(16)	Rh8–B3	2.202(16)
Rh2–B6	2.16(3)	Rh5–B5	2.227(16)	Rh8–B2	2.214(16)
Rh2–B2	2.208(16)	Rh5–B4	2.268(17)	Rh8–B2	2.431(17)
Rh2–B3	2.372(16)	Rh5–B4	2.390(17)	Rh8–Rh8	2.662(2)
Rh2–Rh7	2.6764(19)	Rh5–Rh4	2.799(2)	Rh8–Rh4	2.7073(18)
Rh2–Rh8	2.759(2)	Rh5–Rh3	2.8055(18)	Rh8–Rh7	2.738(2)
Rh2–Rh1	2.7597(18)	Rh5–Rh3	2.8260(18)	Rh8–Rh2	2.759(2)
Rh2–Rh4	2.7765(19)	Rh5–Rh1	2.828(2)	Rh8–Rh4	2.7963(18)
Rh2–Rh1	2.778(2)	Rh5–Rh8	2.858(2)	Rh8–Rh7	2.8352(18)
Rh2–Rh6	2.797(2)	Rh5–Rh6	2.883(2)	Rh8–Rh5	2.858(2)
Rh2–Rh9	2.8065(18)	Rh5–Rh7	2.9212(18)	Rh8–Rh9	2.944(2)
Rh2–Rh6	2.8760(18)	Rh5–Rh6	2.930(2)		
Rh2–Rh9	2.8871(18)				
Rh3–B4	2.132(17)	Rh6–B4	2.166(16)	Rh9–B6	1.98(3)
Rh3–B5	2.139(16)	Rh6–B3	2.195(16)	Rh9–B3	2.077(16)
Rh3–B1	2.165(15)	Rh6–B4	2.195(16)	Rh9–B1	2.168(15)
Rh3–B3	2.199(16)	Rh6–B6	2.23(3)	Rh9–Rh7	2.703(2)
Rh3–B2	2.250(16)	Rh6–Rh9	2.721(2)	Rh9–Rh6	2.721(2)
Rh3–Rh4	2.755(2)	Rh6–Rh7	2.774(2)	Rh9–Rh4	2.758(2)
Rh3–Rh1	2.779(2)	Rh6–Rh1	2.7926(18)	Rh9–Rh1	2.771(2)
Rh3–Rh9	2.7893(19)	Rh6–Rh2	2.797(2)	Rh9–Rh3	2.7893(19)
Rh3–Rh5	2.8055(18)	Rh6–Rh1	2.8001(19)	Rh9–Rh2	2.8065(18)
Rh3–Rh7	2.8062(18)	Rh6–Rh2	2.8760(18)	Rh9–Rh4	2.879(2)
Rh3–Rh5	2.8260(18)	Rh6–Rh5	2.883(2)	Rh9–Rh2	2.8871(18)
Rh3–Rh6	2.965(2)	Rh6–Rh5	2.930(2)	Rh9–Rh8	2.944(2)
		Rh6–Rh3	2.965(2)		

introduced for B6 atom that resulted in the decreasing of R_1 value from 4.30% to 4.18% and 4.10% to 4.01% as well as U_{iso} for B6 atom for both crystals. The results were checked for additional symmetry with assistance of PLATON program package [18]. The final residuals for both the crystals are given in Table 2. The atomic coordinates were standardized using the Structure Tidy program [19] and listed in Table 3. The anisotropic thermal parameters for Rh atoms are presented in Table 4. The crystal structure of the Rh_3B_{2-x}, $x = 0.167$ compound is shown in Fig. 1.

4. Discussion

The crystal structure of the compound belongs to the new structure type of intermetallic compounds and is the first representative of structures with triclinic symmetry among binary borides.

Interatomic distances for Rh atoms are shown in Table 5. Coordination polyhedra for these atoms are rather asymmetric and have 12, 13 and 14 vertexes. Minimum and maximum Rh–Rh distances are 2.6597 and 2.9645 Å, respectively. Those slightly larger than the sum of radii [20] distances have been also encountered for several compounds from the R–B system, $d_{Rh-Rh} = 2.591 - 3.034$ Å for Rh_7B_3 and $d_{Rh-Rh} = 2.697 - 3.306$ Å for Rh_5B_4 as well as 2.845 Å for $RhB_{1.1}$.

According to classification of Krypyakevych [21], this structure belongs to class N10. The coordination polyhedra for B atoms are trigonal prisms, which are formed by six rhodium atoms without or with 1, 2 or 3 additional atoms (Fig. 2). Some of the interatomic Rh–B distances (Table 6) are shorter as compared with the atomic radii sum of 2.22 Å; however, these values are not unusual for borides. A number of platinum metal borides also display short metal–B distances, e.g. Rh_5B_4 with Rh–B distances of 2.080 and 2.148 Å, $IrB_{0.9}$ and $IrB_{1.35}$ with $d_{Ir\text{-}B} = 2.04-2.13$ Å (radii sum 2.24 Å) and Pd_2B with $d_{Pd\text{-}B} = 2.104-2.122$ Å (radii sum 2.25 Å). The smallest value of Rh–B bond length in Rh_3B_{2-x}, $x = 0.167$ structure, 1.98(6) Å, was observed for Rh9–B6 verifying the partial occupancy of the atomic position by B6 atom as obtained from the structural refinement.

The classification scheme based of the type of boron–boron aggregation within complex metal borides have been presented by different group of authors [21,22]. This classification can be achieved in terms of the boron–boron aggregation which turns out to be function of the boron concentration. The decision, as to which specific type of B–B aggregation occurs, depends on the distances between boron atoms. In the YB_{66}, NaB_{15}, AlB_{12}, CaB_6, ThB_4 structure types boron atoms form three-dimensional boron frameworks. In the AlB_2, ReB_2, RuB_2 structures they form two-dimensional boron nets. The structures of the V_2B_3, V_5B_6, FeB, CrB, MoB, PtB compounds can be considered as chain borides.

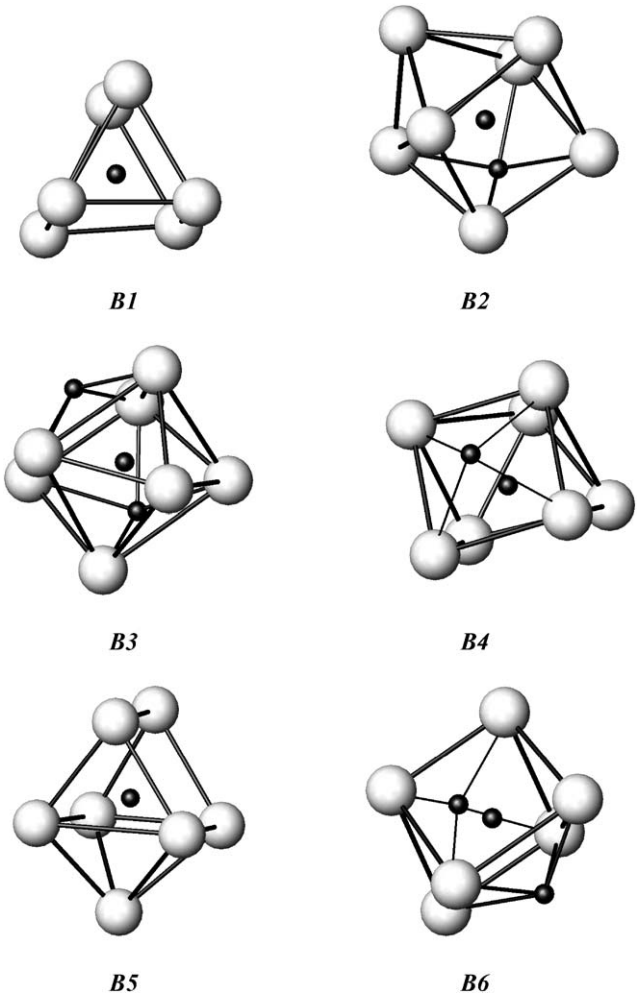

Fig. 2. Coordination polyhedra of boron atoms in the Rh_3B_{2-x} structure.

In the case of the Rh_3B_{2-x}, $x = 0.167$ compound we observed three different types of the boron–boron aggregation (Fig. 3):

1. isolated boron atoms, namely B1 and B5
2. B–B pairs
3. B_6 chain fragments

Isolated B atoms are typical for the structures with poor concentration of boron (Table 7). The ratio between metal and boron atoms for two Cr_5B_3 and $(W,Fe)_3B_2$ compounds is very close to those in Rh_3B_{2-x}, $x = 0.167$ and all of these three structures contain boron pairs with B–B distances $d = 1.86$ Å. A B_4 chain fragment with $d_{B-B} = 1.82-1.83$ Å was observed in the Mo_2IrB_2 structure. Similar interatomic distances between four boron atoms (B3–B6–B6–B3) in the inner section of the B_6 chain fragment are 1.82(4)–1.86(6) Å

Table 6
Selected interatomic distances (d, Å) for the B atoms in Rh_3B_{2-x} structure

Atom	d, Å	C.N.	Atom	d, Å	C.N.
B1–Rh2	2.100(15)	6	B4–B4	1.86(3)	8
B1–Rh5	2.133(15)		B4–Rh3	2.132(17)	
B1–Rh3	2.165(15)		B4–Rh1	2.152(17)	
B1–Rh9	2.168(15)		B4–Rh6	2.166(16)	
B1–Rh4	2.175(16)		B4–Rh6	2.195(16)	
B1–Rh4	2.216(16)		B4–Rh5	2.268(17)	
B2–B3	2.00(2)	8	B4–Rh5	2.390(17)	
B2–Rh7	2.104(16)		B4–Rh1	2.629(16)	
B2–Rh5	2.140(16)		B5–Rh7	2.124(15)	7
B2–Rh2	2.208(16)		B5–Rh8	2.137(15)	
B2–Rh8	2.214(16)		B5–Rh3	2.139(15)	
B2–Rh3	2.250(16)		B5–Rh4	2.215(15)	
B2–Rh1	2.290(17)		B5–Rh5	2.227(16)	
B2–Rh8	2.431(17)		B5–Rh4	2.228(15)	
B3–B6	1.82(4)	9	B5–Rh7	2.407(15)	
B3–B2	2.00(2)		B6–B3	1.82(4)	8
B3–Rh9	2.077(16)		B6–B6	1.86(6)	
B3–Rh6	2.195(16)		B6–Rh9	1.98(3)	
B3–Rh3	2.199(16)		B6–Rh2	2.04(3)	
B3–Rh8	2.202(16)		B6–Rh2	2.16(3)	
B3–Rh7	2.205(16)		B6–Rh1	2.18(3)	
B3–Rh2	2.372(16)		B6–Rh6	2.23(3)	
B3–Rh1	2.392(16)		B6–Rh1	2.28(3)	

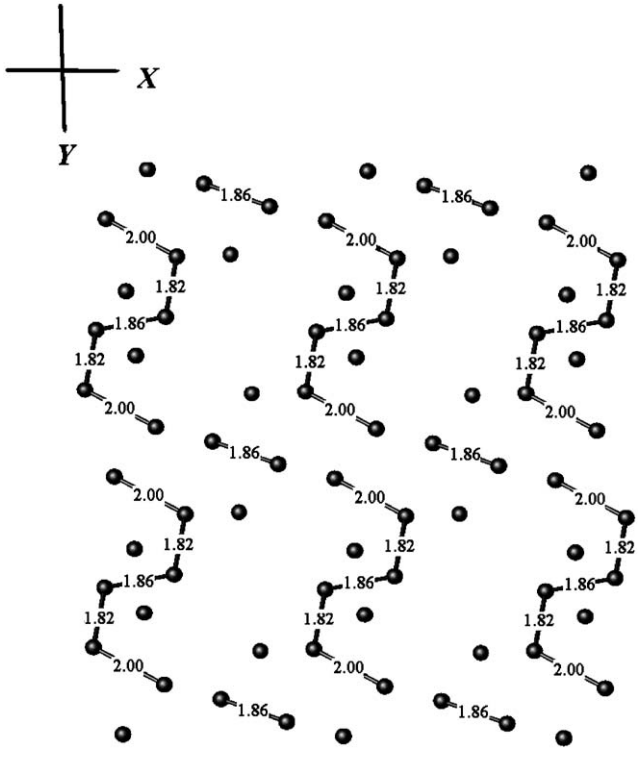

Fig. 3. Three types of B–B aggregation in the Rh_3B_{2-x} structure.

and two outer B2 atoms are located at rather longer distance of 2.00(2) Å. This value is large if compared with the radii sum but is smaller than the B–B distances for boron chain fragment in the Rh_5B_4 compound ($d_{B-B} = 2.22$ Å).

Table 7
Classification of the borides with metal–boron ratio from 3/1 to 3/2 [22,23]

Compound	Aggregation of boron atoms
Re_3B (Ti_3P str. type), Pd_3B (Fe_3C str. type)	Isolated boron atoms
Pd_5B_2 (Mn_5C_2 str. type)	Isolated boron atoms
Rh_7B_3 (Th_7Fe_3 str. type)	Isolated boron atoms
Ta_2B ($CuAl_2$ str. type), Cr_2B (Mg_2Cu str. type), Pd_2B (anti-$CaCl_2$ str. type)	Isolated boron atoms
Cr_5B_3 (own str. type)	Isolated boron atoms and boron pairs
$(W,Fe)_3B_2$ (U_3Si_2 str. type)	Boron pairs
Mo_2IrB_2 (Y_3Co_2 str. type)	B_4 chain fragments

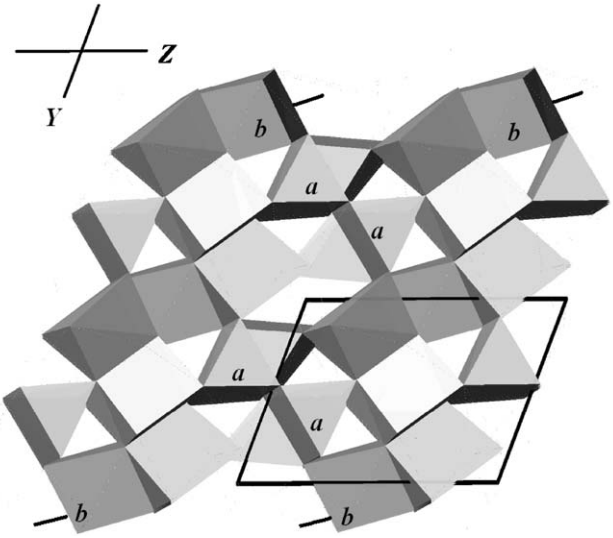

Fig. 4. Arrangement of trigonal prisms in the Rh_3B_{2-x} structure.

The structure can be described as built up from boron centered slightly deformed trigonal prisms formed by rhodium atoms. The [B1Rh_6] and [B5Rh_6] trigonal prisms form chains in the [1 0 0] direction (Fig. 4a) and the other ones build the three dimensional zig-zag chains (Fig. 4b). The holes which are formed between these two types of arrangement of trigonal prisms can be occupied by atoms with smaller size (e.g. C or N).

Acknowledgments

O.S. is grateful to Austrian FWF for the Lise Meitner Grant (Project M635). This work was partially supported by FCT (Portugal) under contract No. POCTI/

QUI/46066/2002. The authors express their thanks to Prof. P. Rogl, Institut für Physikalische Chemie, Universität Wien for the use of the Image Plate Huber G 670 diffractometer.

Supporting information: Further details of the crystal structure investigation can be obtained from the Fachinformationszentrum Karlsruhe, 76344 Eggenstein-Leopoldshafen,Germany (fax: (49) 7247-808-666, e-mail:crysdata@fiz.karlsruhe.de) on quoting the depository number for Rh_3B_{2-x} compound is CSD 413800.

References

[1] T.S. Massalski, Binary Alloy Phase Diagrams, 2nd Edition, American Society for Metals, Metals Park, OH, 1990.
[2] V.A. Kosenko, B.M. Rud, V.G. Sidorova, Inorg. Mater. 7 (1970) 1294.
[3] G. Reinacher, Rev. Metal. 54 (1957) 321.
[4] B. Aronsson, E. Stenberg, J. Aselius, Acta Chem. Scand. 14 (1960) 733.
[5] R.W. Mooney, A.J.E. Welch, Acta Crystallogr. 7 (1954) 49.
[6] B.I. Nolang, L.-E. Tergenius, I. Westman, J. Less-Common Met. 82 (1981) 303.
[7] T. Roisnel, J. Rodriguez-Carvajal, WinPLOTR, a tool to plot powder diffraction patterns, Laboratoire Leon Brillouin (CEA-CNRS), France, 1998.
[8] G. Nolze, W. Kraus, PowderCell 2.3 Program, BAM Berlin, 2000.
[9] P.-E. Werner, L. Eriksson, M. Westdahl, J. Appl. Crystallogr. 18 (1985) 367.
[10] D. Boultif, D. Louer, J. Appl. Crystallogr. 24 (1991) 987.
[11] SMART, SAINT, and SADABS Packages, Version 5.1, Bruker AXS, Madison,WI, USA, 1997–1999.
[12] L.J. Farrugia, J. Appl. Crystallogr. 32 (1999) 837.
[13] R.E. Marsh, Acta Crystallogr. B 51 (1995) 897.
[14] P. McArde, J. Appl. Crystallogr. 29 (1996) 306.
[15] G.M. Sheldrick, SHELXS-97, Program for the Solution of Crystal Structures, University of Göttingen, Germany, 1997.
[16] T. Hahn (Ed.), International Tables for Crystallography, Vol. A, Space Group Symmetry, D. Reidel, Dordrecht, 1983.
[17] G.M. Sheldrick, SHELXL-97. Program for the Crystal Structure Refinement, University of Göttingen, Germany, 1997.
[18] A.L. Spek, J. Appl. Crystallogr. 36 (2003) 7.
[19] E. Parthé, K. Cenzual, R. Gladyshevskii, J. Alloys Compd. 197 (1993) 291.
[20] W.B. Pearson, Crystal Chemistry and Physics of Metals and Alloys, Vol. 1, Mir, Moscow, 1977.
[21] P.I. Krypyakevich, Structure Types of Intermetallic Compounds, Nauka, Moskva, 1977, p. 287.
[22] P. Rogl, H. Nowotny, J. Less-Common Met. 61 (1978) 39.
[23] Yu.B. Kuz'ma, Crystal Chemistry of Borides, Vyshcha Shkola Press, Lvov, 1983.